GEOPHYSICS, VOL. 62, NO. 6 (NOVEMBER-DECEMBER 1997); P. 1724–1729, 5 FIGS.

1-D inversion of resistivity and induced polarization data for the least number of layers

Francisco J. Esparza* and Enrique Gómez-Treviño*

ABSTRACT

An automatic inverse method has been developed for generating layered earth models from electrical sounding data. The models have the minimum number of layers required to fit a resistivity sounding curve or a combined resistivity and induced polarization sounding. The ground is modeled using a very large number of thin layers to accommodate arbitrary variations. The properties of the layers are optimized using as a constraint the L_1 norm of the vertical derivative of the resistivity distribution. The use of linear programming leads to piecewise smooth distributions that simulate traditional models made up of a few uniform layers. The process considers from the simplest model of a uniform halfspace to models of many layers, without fixing a priori the number of discontinuities. The solution is sought by iterating a new linear approximation, similar to the classical process of linearization, except that a reference model is not present in either the data vector or the unknown function. For induced polarization soundings, the problem is linear and the solution is obtained in a single iteration, provided an adequate resistivity model is available. The performance of the method is illustrated using numerical experiments and published deep resistivity data from Australia. The method also is applied to combined resistivity and induced polarization soundings from a local groundwater prospect in México.

INTRODUCTION

All existing methods to interpret electrical soundings in terms of 1-D resistivity variations fall in one of two groups, depending on how these variations are considered as a function of depth. In the first and more traditional group, the earth is divided into a small number of layers whose resistivities and thicknesses are to be determined from the sounding data. This can be done visually using master curves (e.g., Orellana and Mooney, 1966) or using automatic curve-fitting algorithms (e.g., Inman, 1975). The outcome of the interpretation is a layered-earth model made up of a few homogeneous layers. In most geological situations, this is the best model of the earth, so many interpreters favor the methods in this group. The decision as to the number of layers is left to the interpreter. Although this can be used to advantage by experienced users, in general it represents a subjective judgment that makes the interpretation user dependent.

In the second group of methods, the need for external information is minimized. The vertical resistivity distribution is represented by an arbitrary function of depth or, equivalently, the earth is divided into many thin layers to approximate continuous variations. The resistivities of the thin layers are optimized in some way to produce models that vary smoothly with depth (e.g., Oldenburg, 1978; Constable et al., 1987; Zohdy, 1989). The form of the resulting function automatically reflects the locations and the electrical properties of relevant layers buried in the earth. The methods are robust and require no external information on the number of highs and lows of the resistivity function. However, the critics of this approach argue that for most geological situations, a smooth variation of resistivity with depth is less adequate than the traditional representation of a small number of homogeneous layers. For this reason, the continuous models are sometimes used only as a guide in traditional interpretations. For example, the algorithm developed by Zohdy (1989) allows the user to propose simple layered models on the basis of the automatically generated continuous distributions.

In this paper, we present a method that combines features from each of the two groups described above. The objective is to obtain traditional models composed of a small number of homogeneous layers without having to specify this number a priori, so that the interpretation process is free from this external information and is as automatic as possible. We have been using this method successfully for the routine interpretation of

Manuscript received by the Editor November 16, 1995; revised manuscript received February 7, 1997.
*Division de Ciencias de la Tierra, Centro de Investigación Científica y de Educación Superior de Ensenada, Km. 107 Carr. Tijuana-Ensenada, Ensenada, Baja California, 22860 Mexico. E-mail: fesparz@cicese.mx; egomez@cicese.mx.

combined resistivity and induced polarization (IP) soundings. Here we describe the basis of the method and present some of the applications.

THEORY

There are many ways of approaching resistivity inverse problems. We have chosen the framework given in Gómez-Treviño (1987a) for electromagnetic inverse problems, because it offers the possibility of exploring alternatives to traditional methods and because it applies equally to problems in higher dimensions. It has long been recognized that the more the stock of solution methods is increased, the better the scope of solutions sampled when dealing with nonlinear inverse problems. Regarding the integral equations derived in Gómez-Treviño (1987a), no known numerical solution has been implemented for the full nonlinear problem. The solution presented here is the first known successful attempt, although the equations have been used to develop 2-D imaging techniques for dc resistivity and magnetotelluric measurements (Pérez-Flores and Gómez-Treviño, 1997; Romo et al., 1997) and as a theoretical framework to approach inversion-related problems (Gómez-Treviño, 1987b; Esparza and Gómez-Treviño, 1987; Sasaki, 1989; Spies, 1989; Boerner and Holladay, 1990). Dosso and Oldenburg (1991) tried the formulation for the 1-D magnetotelluric problem but encountered some apparent difficulties that prevented them from making any practical use of the integral formulation. The solution presented here overcomes some of these difficulties. The remaining questions are addressed in Esparza and Gómez-Treviño (1996) for issues specific to the magnetotelluric problem.

For electric field measurements in the time domain, the integral equation is

$$E_i + t\frac{\partial E_i}{\partial t} = -\int_0^\infty G_i(z,\sigma)\sigma(z)\,dz. \tag{1}$$

E_i stands for the electric field at the surface, t is time, σ is electrical conductivity, and G_i is the Fréchet derivative of E_i with respect to σ. In what follows, we assume that the measurements correspond to a standard dc Schlumberger array. Apparent resistivity ρ_a is related to the electric field by

$$\rho_a(r_i) = \pi r_i^2 \frac{E_i}{I}, \tag{2}$$

where $r_i = AB/2$. AB is the distance between the outer-current electrodes, and I is the current driven into the earth. Because we are concerned with dc measurements, the partial derivative in equation (1) is equal to zero. It is easy to see that equation (1) also is valid for apparent resistivity. That is,

$$\rho_a(r_i) = -\int_0^\infty G_i(z,\sigma)\sigma(z)\,dz, \tag{3}$$

where G_i is the Fréchet derivative of ρ_a with respect to σ. If H is the Fréchet derivative of ρ_a with respect to ρ, equation (3) transforms to

$$\rho_a(r_i) = \int_0^\infty H_i(z,\rho)\rho(z)\,dz. \tag{4}$$

This equation also is valid when $\rho_a(r_i)$ and $\rho(z)$ are replaced by $\delta\rho_a(r_i)$ and $\delta\rho(z)$, respectively. In fact, the result is the familiar linearized equation that has been used for the inversion of resistivity data (Oldenburg, 1978). Here, $\delta\rho_a(r_i)$ and $\delta\rho(z)$ represent perturbations around a reference model. The interesting feature about equation (4) is that it relates $\rho(z)$ directly to ρ_a regardless of a reference model. Our intention is to solve equation (4) iteratively for the unknown electrical resistivity without considering perturbations.

For control reasons, we use the logarithm of apparent resistivity and resistivity in the inversion code. This is done by multiplying and dividing by $\log\rho(z)$ within the integral sign and by $\log\rho_a(r_i)$ on the left side of equation (4). The resulting equation can be written as

$$\log\rho_a(r_i) = \int_0^\infty \left[\frac{\rho(z)}{\rho_a(r_i)}\frac{\log\rho_a(r_i)}{\log\rho(z)}H_i(z,\rho)\right]\log\rho(z)\,dz. \tag{5}$$

NUMERICAL PROCEDURE

The general idea is to iterate equation (5) starting from a uniform half-space and then at each iteration to update the term in brackets. At each iteration, $\log\rho(z)$ is obtained from $\log\rho_a(r_i)$ until the model fits the data to a required level.

The idea of applying linear programming to the present nonlinear problem came from its success in linear situations. For low-resistivity contrast, the inverse 1-D IP problem is linear with respect to chargeability (Esparza and Gómez-Treviño, 1989). The same is true for arbitrary 1-D conductivity variations when considering electromagnetic measurements at low induction numbers (Esparza and Gómez-Treviño, 1987; Esparza, 1991; Cheesman and Bailey, 1992). In both cases, the inverse problem can be formulated in terms of a linear integral equation that can be solved directly using linear programming techniques. It is possible in these cases to obtain traditional layered-earth models made up of a few homogeneous layers without specifying their number a priori. The idea here is to apply iteratively the same procedure to the nonlinear resistivity problem. For the sake of simplicity, we use equation (4) in the algebraic steps that follow. The result applies equally to the logarithmic version [equation (5)].

We are interested in minimum-structure solutions. Therefore, we follow Oldenburg and Samson (1979), who applied a similar technique to a linear problem with interferometric data. Integrating equation (4) by parts, the result is

$$\rho_a(r_i) - \rho(0)T_i(0) = \int_0^\infty T_i(z,\rho)\rho'(z)\,dz, \tag{6}$$

with

$$T_i(z,\rho) = \int_z^\infty H_i(u,\rho)\,du. \tag{7}$$

To solve equation (6) numerically, we divide the depth axis into a large number m of thin layers so that the integral can be converted into a sum. The algebraic details are given in the Appendix. The result is

$$\rho_a(r_i) = \sum_{j=1}^{m-1}\left[\sum_{\ell=j+1}^{m}\frac{\partial\rho_a(r_i)}{\partial\rho_\ell}\right](\rho_{j+1}-\rho_j) + \rho_1\sum_{j=1}^{m}\frac{\partial\rho_a(r_i)}{\partial\rho_j}, \qquad i = 1,n, \tag{8}$$

where n is the number of measurements. We consider that $m > n$ and ρ_j is the resistivity of the jth thin layer.

To find the solution of equation (8), we use the L_1 norm and minimize the objective function

$$\phi = \sum_{j=1}^{m-1} |\rho_{j+1} - \rho_j|. \tag{9}$$

Equation (8) can be written in a matrix form as

$$\mathbf{y} = \mathbf{Ax}. \tag{10}$$

Given that the apparent resistivities have an associated error, e.g., e_i, instead of solving equation (10) exactly, we solve the system of inequalities

$$\mathbf{y} - \mathbf{e} \leq \mathbf{Ax} \leq \mathbf{y} + \mathbf{e}. \tag{11}$$

The unknowns of the problem are the resistivities of the thin layers. The number of these layers and their thicknesses are kept constant. The idea is that by optimizing ϕ, many of the resistivities of the thin layers will have the same value, resulting in models with a minimum number of discontinuities. The whole problem, the solution of the system of inequalities (11) subject to the minimization of ϕ, can be solved by means of standard linear programming techniques (Gass, 1969). We compute $\rho_a(r_i)$ using the digital filters of Johansen (1975). In the calculation of the partial derivatives, we follow Constable et al. (1987). The inversion code can be implemented easily using the linear programming package included in Press et al. (1992).

For the inversion of IP data, we use the formulation given in Seigel (1959), which relates the apparent chargeability $m_a(r_i)$ to the chargeability m_j of the jth layer in a linear way. The expression is

$$m_a(r_i) = \sum_{j=1}^{m} \frac{\partial \log \rho_a(r_i)}{\partial \log \rho_j} m_j. \tag{12}$$

If the resistivity model is known, then the inversion of IP data is linear. To find the chargeability vector **m**, we use the same procedure as that described for the resistivity data. The only difference is that for the present case, the chargeability model is obtained in a single iteration and there is no need to use logarithmic scaling.

To initiate the solution of the system of inequalities (11), we use a homogeneous half-space to compute **A** and solve for **x**. This is done in the following way. We solve the system (11) using $k\mathbf{e}$ as the error vector and monitor the rms misfit

$$\text{rms}^2 = \frac{1}{n} \sum_{i=1}^{n} \left[\frac{\log \rho_a(r_i) - \log \hat{\rho}_a(r_i)}{e_i} \right]^2 \tag{13}$$

as a function of k; $\hat{\rho}_a$ stands for the calculated apparent resistivity. We select the model for which the rms misfit is minimum. With the resulting model, we compute a new **A** and solve for **x** again. The process is iterated until the model fits the data to the required level. $T_i(z, \rho)$ for a homogeneous half-space does not depend on the resistivity itself (Oldenburg, 1978). This implies that our final model in the iterative process is independent of the resistivity assigned to the initial half-space, since this value never enters into the computations. Figure 1 shows how the iterative process converges for synthetic data with no errors.

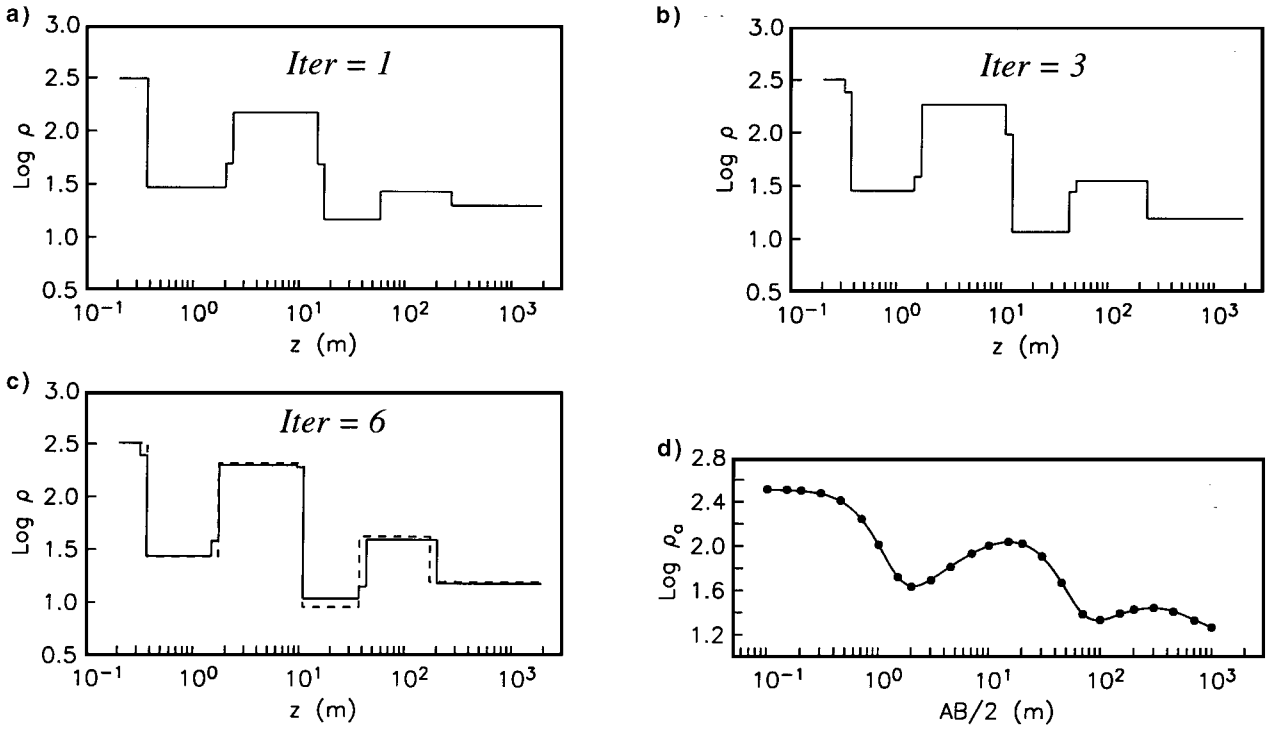

FIG. 1. Application of the inversion method to synthetic data. The broken line in (c) represents a hypothetical model whose response was sampled, as shown by the solid dots in (d). The sampled response was inverted to produce the models shown in (a), (b), and (c), which correspond to the first, third, and sixth iterations, respectively. The sampled response is noise free, but the corresponding values were assumed to have errors of 1%. The algorithm converged after six iterations to a value of rms = 1.0. The continuous line in (d) represents the response of the final model.

The system of inequalities (11) was formed assuming errors of 1%, so the sounding curve was fit to a 1% level.

In Figure 1, at the first iteration the algorithm picks up the basic structure of the six-layer model. The interfaces that define the different layers automatically appear when plotting at this stage the solution of the system of inequalities. Regarding the final model obtained after six iterations, it must be observed that some of its interfaces seem to require more iterations to sharpen the definition of the layers. There are small-scale variations that are unlikely to be resolved by the data but, strictly speaking, must be considered as extra layers in the model. These layers are always very thin, and their resistivity is intermediate, corresponding to that of a transition zone, so there is very little cause for confusion. They must be considered simply as transition zones between the actual layers of the model. A few numerical experiments indicated that the thicknesses of these transition layers depend only on the discretization of the depth axis. If required, the definition of the interfaces can be sharpened by making this discretization finer. This is illustrated in Figure 2 for four different discretizations.

An interesting problem arises when the resistivity value of one or more layers is close to 1 $\Omega \cdot$ m. In this case, the term in brackets in equation (5) may become unbounded and thus difficult to handle numerically. The system of inequalities (11) becomes unstable, and the iterative process fails to converge. For this reason, in the event that values of resistivity near 1 $\Omega \cdot$ m are suspected, it is recommended that all the resistivities in the model as well as the apparent resistivity data be scaled up to different units. A factor of 10 will shift most real sounding curves well above the dangerous point.

APPLICATIONS

In this section, we apply the methodology described above to field data. For the first application, we used the resistivity data described in Constable et al. (1984), which correspond to a long-offset sounding made in the central Australian shield. The relative error in the apparent resistivity data reported in Constable et al. (1987) is about 10%. The estimated model after 14 iterations is presented in Figure 3b; the corresponding model response is shown in Figure 3a. The normalized rms was 1.0. In Figure 3b, together with our model, we include the resistivity model obtained by Constable et al. (1987) using Occam's philosophy. The agreement between the two models is reasonably good. However, our model is easier to relate to a traditional stratified earth. Nevertheless, both models fit the data and, in the absence of additional information, both must be considered as acceptable models of the earth.

In a second example, we interpreted data described by Vega (1989), who used a combined study of resistivity and IP soundings to determine the boundary between a fresh aquifer and saline intrusion from the sea. The study was made in a farming region near Ensenada, México. We estimated the relative uncertainty in the apparent resistivity data to be 5%. The model found in two iterations is presented in Figure 4a. The corresponding rms for this model is 1.0. The model response is shown in Figure 4a. The IP sounding is presented in Figure 4b, together with the chargeability model. It is worth noting that the resistivity model shows very little character as compared with the corresponding IP model. The data and the models shown in Figure 5 correspond to a site at which there exist both resistivity

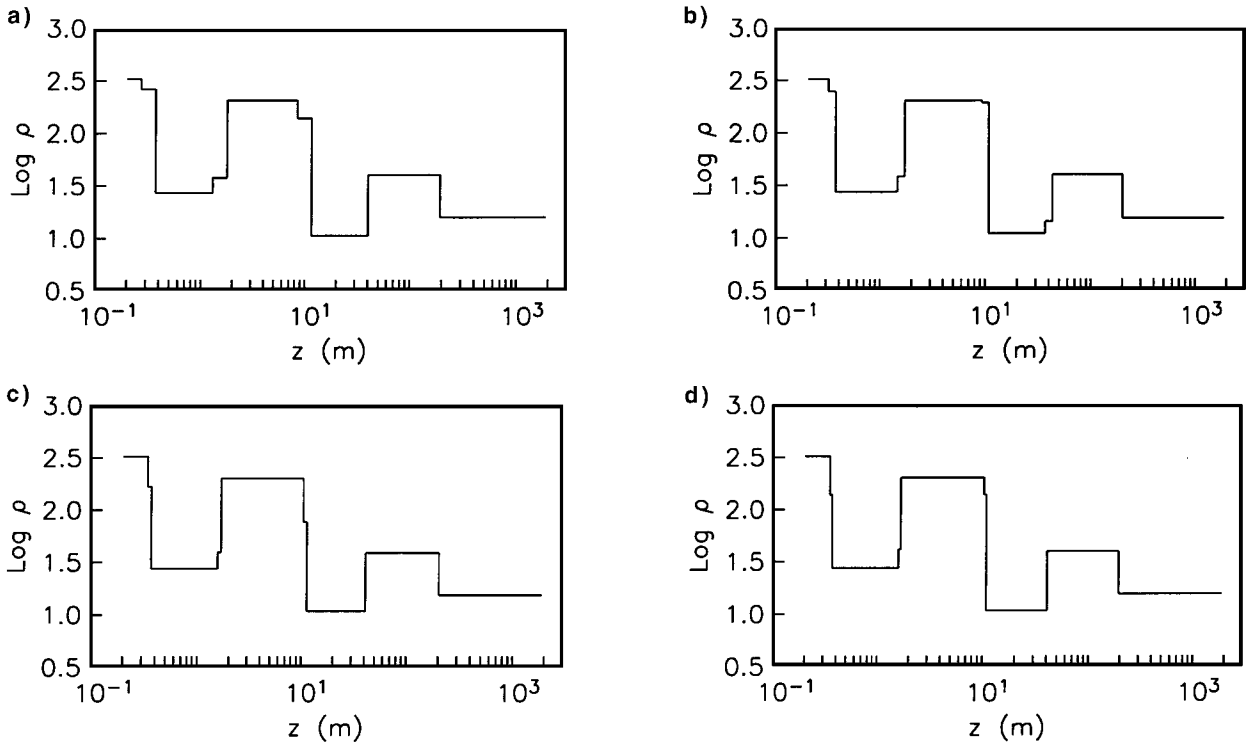

FIG. 2. Final models for four different discretizations of the depth axis. The models were obtained in six iterations using as data the sounding curve shown in Figure 1d. In all cases, the discretization begins at a depth of 0.2 m and ends at 1700 m. The intermediate depths follow geometric series defined by m, the number of unknowns. The models correspond to (a) $m = 30$, (b) $m = 60$, (c) $m = 120$, and (d) $m = 180$. The model shown in Figure 1 was obtained using $m = 60$.

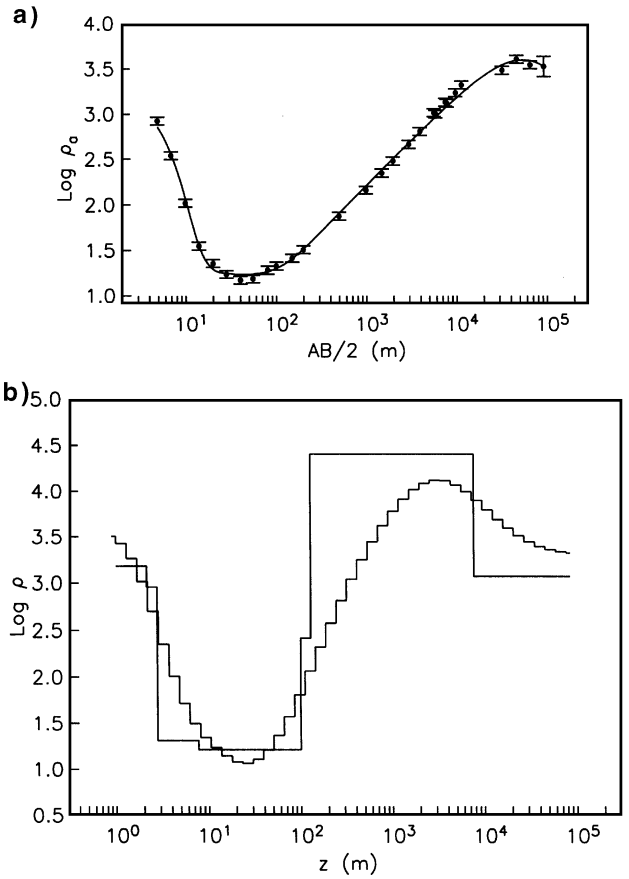

FIG. 3. Application of the inversion method to field data. (a) Comparison of resistivity sounding data (isolated points) with the response of our final layered-earth model (continuous line). The data are taken from Constable et al. (1984). (b) Comparison of our final layered-earth model with the smooth profile obtained by Constable et al. (1987) using Occam's philosophy. In both cases, the fit to the data is such that rms = 1.0. In the present case, the final model was obtained after 14 iterations.

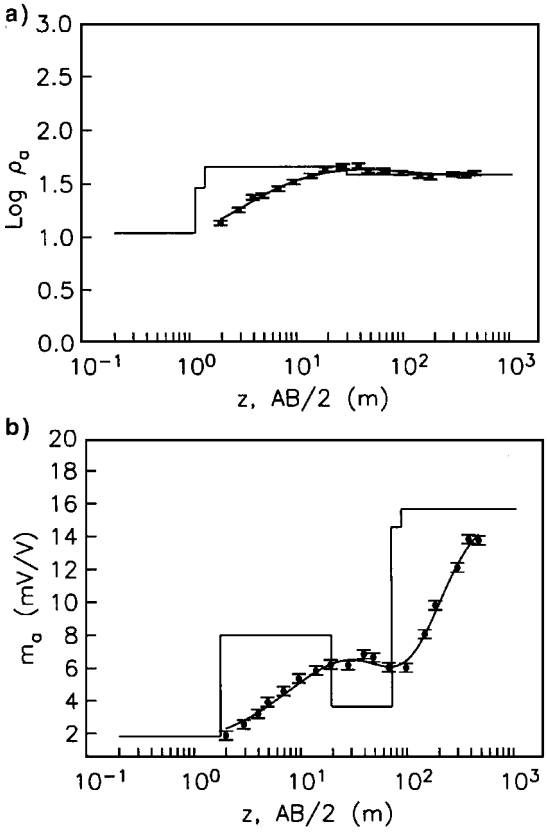

FIG. 4. Interpretation of a combined resistivity and IP sounding. (a) Comparison of the resistivity data with the response of the corresponding final model. The resistivity model is plotted using the same scale as the data. (b) Comparison of the IP sounding for the same site with the response of the IP model. The IP model is plotted using the same scale as the IP data. At this site, there is almost no contrast in resistivity. The IP model shows boundaries not available in the resistivity sounding. The resistivity model was obtained in two iterations, and the IP model was obtained in one.

and IP contrasts at depth. The correlation of the resistivity and IP boundaries helped to distinguish between saline water strata and clay layers, because both present similar resistivity values, but their IP responses are quite different.

CONCLUSIONS

In this paper, we have applied a nonlinear integral equation to the interpretation of resistivity soundings. The proposed iterative approach, which is different from classical linearization, converges well for the examples shown. The method does not strictly require the use of the approximation that we describe here. In fact, it could be implemented using traditional linearization. We have chosen to explore other alternatives with the hope of increasing the scope of possible solutions. By imposing minimum L_1 structure, we have found simple stratified models that should appeal to traditional interpreters of resistivity sounding data. The method is automatic and does not require a priori specification of the number of layers of the model. This is accomplished by considering a large number of thin layers whose resistivities are optimized using linear programming techniques. The results are piecewise uniform distributions that simulate traditional stratified models made up of a few homogeneous layers.

ACKNOWLEDGMENTS

We thank the reviewers of the manuscript for their helpful comments.

REFERENCES

Boerner, D. E., and Holladay, J. S., 1990, Approximate Fréchet derivatives in inductive electromagnetic soundings: Geophysics, **55**, 1589–1595.

Cheesman, S., and Bailey, R. C., 1992, L_1 model norm inversion of electromagnetic data: A demonstration using EM-34 resistive limit data: Presented at the 11th IAGA Workshop on Electromagnetic Induction in the Earth.

Constable, S. C., McElhinny, M. W., and McFadden, P. L., 1984, Deep Schlumberger sounding and the crustal resistivity structure of central Australia: Geophys. J. Roy. Astr. Soc., **79**, 893–910.

Constable, S. C., Parker, R. L., and Constable, C. G., 1987, Occam's inversion: A practical algorithm for generating smooth models from electromagnetic sounding data: Geophysics, **52**, 289–300.

Dosso, S. E., and Oldenburg, D. W., 1991, The similitude equation in magnetotelluric inversion: Geophys. J. Internat., **106**, 507–509.

Esparza, F. J., 1991, Sufficiency of Maxwell's equations in relation with electromagnetic inverse problems: Ph.D. thesis, Centro de Investigación Científica y de Educación Superior de Ensenada.

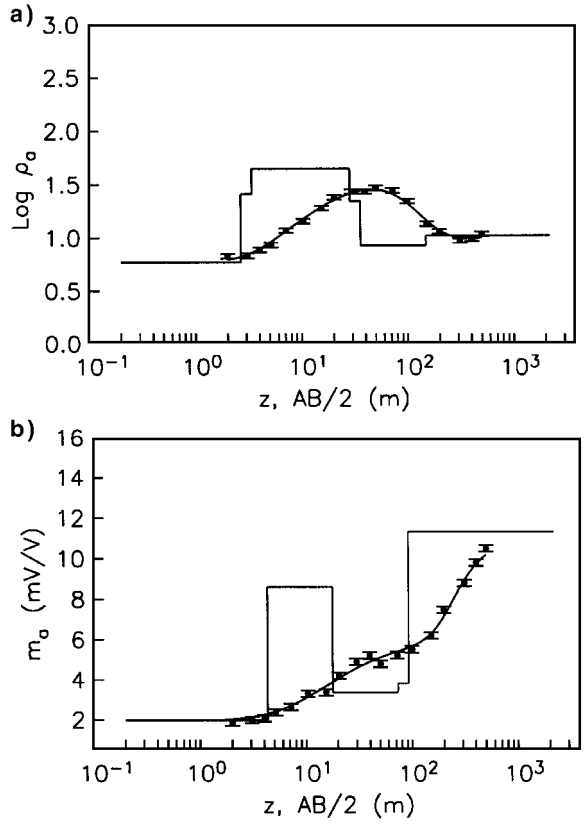

FIG. 5. Interpretation of a combined resistivity and IP sounding. This case differs from the one shown in Figure 4 in that the present resistivity curve has more character. (a) Resistivity data compared with the response of the final resistivity model. (b) IP data compared with the response of the IP model. In both cases, the models are plotted using the same scales as their corresponding data sets. The resistivity model was obtained in three iterations, and the IP model was obtained in one.

Esparza, F. J., and Gómez-Treviño, E., 1987, Electromagnetic sounding in the resistive limit and the Backus-Gilbert method for estimating averages: Geoexpl., **24**, 441–454.

——— 1989, Inversión unidimensional de datos de polarización inducida para medios con contraste pequeño en resistividad: Geofís. Internac., **28**, 467–479.

——— 1996, Inversion of magnetotelluric soundings using a new integral form of the induction equation: Geophys. J. Internat., **127**, 452–460.

Gass, S. L., 1969, Linear programming: McGraw-Hill Book Co.

Gómez-Treviño, E., 1987a, Nonlinear integral equations for electromagnetic inverse problems: Geophysics, **52**, 1297–1302.

——— 1987b, A simple sensitivity analysis of time-domain and frequency-domain electromagnetic measurements: Geophysics, **52**, 1418–1423.

Inman, J. R., 1975, Resistivity inversion with ridge regression: Geophysics, **40**, 798–817.

Johansen, H. K., 1975, An interactive computer/graphic-display terminal system for interpretation of resistivity soundings: Geophys. Prosp., **23**, 449–458.

Oldenburg, D. W., 1978, The interpretation of direct current resistivity measurements: Geophysics, **43**, 610–625.

Oldenburg, D. W., and Samson, J. C., 1979, Inversion of interferometric data from cylindrically symmetric, refractionless plasmas: J. Opt. Soc. Am., **69**, 927–942.

Orellana, E., and Mooney, H. M., 1966, Master tables and curves for vertical electrical soundings over layered structures: Interciencia.

Pérez-Flores, M. A., and Gómez-Treviño, E., 1997, Dipole-dipole resistivity imaging of the Ahuachapán-Chipilapa geothermal field, El Salvador, C.A.: Geothermics, Vol. 26.

Press, W. H., Teukolsky, S. A., Vetterling, W. T., and Flannery, B. P., 1992, Numerical recipes in FORTRAN: The art of scientific computing: Cambridge Univ. Press.

Romo, J. M., Flores-Luna, C., Vega, R., Vázquez, R., Pérez-Flores, M. A., Gómez-Treviño, E., Esparza, F. J., Quijano, J. E., and García, V. H., 1997, A closely-spaced magnetotelluric study of the Ahuachapán-Chipilapa geothermal field, El Salvador: Geothermics.

Sasaki, Y., 1989, Sensitivity analysis of magnetotelluric measurements in relation to static effects: Geophys. Prosp., **37**, 395–406.

Seigel, H. O., 1959, Mathematical formulation and type curves for induced polarization: Geophysics, **24**, 547–565.

Spies, B. R., 1989, Depth of investigation in electromagnetic sounding methods: Geophysics, **54**, 872–888.

Vega, M. E., 1989, Combinación de sondeos de resistividad y polarización inducida en el estudio de un acuífero costero: M.Sc. thesis, Centro de Investigación Científica y de Educación Superior de Ensenada.

Zohdy, A. A. R., 1989, A new method for the automatic interpretation of Schlumberger and Wenner sounding curves: Geophysics, **54**, 245–253.

APPENDIX

MATRIX VERSION OF THE INTEGRAL EQUATION

We discretize integral equation (6) to obtain a set of equations and apply linear programming techniques for its solution. Consider a partition $z_1 = 0 < z_2 < z_3 < \cdots < z_m$ in the interval $[0, +\infty]$, where m is the number of layers. Assume that the resistivity is uniform in each subinterval; then, for $z \in (z_j, z_{j+1})$, $\rho(z) = \rho_j$. Consequently, the derivative of $\rho(z)$ can be expressed as a train of delta functions as

$$\rho'(z) = \sum_{j=1}^{m-1} (\rho_{j+1} - \rho_j)\delta(z - z_{j+1}). \qquad \text{(A-1)}$$

Equation (6) is transformed to

$$\rho_a(r_i) - \rho_1 T_i(0) = \sum_{j=1}^{m-1} (\rho_{j+1} - \rho_j) T_i(z_{j+1}, \rho). \qquad \text{(A-2)}$$

Now consider a perturbation in the resistivity of the jth layer. Its contribution to $\delta\rho_a$ is simply $(\partial\rho_a/\partial\rho_j)\Delta\rho_j$. From the linearized equations that involve the Fréchet derivative, the value of $\delta\rho_a$ is $\int_{z_j}^{z_{j+1}} H_i \Delta\rho_j \, dz$, and we obtain

$$\int_{z_j}^{z_{j+1}} H_i(z, \rho)\, dz = \frac{\partial\rho_a(r_i)}{\partial\rho_j}. \qquad \text{(A-3)}$$

Finally, making use of equations (7) and (A–3), equation (A–2) is transformed to

$$\rho_a(r_i) = \sum_{j=1}^{m-1} \left[\sum_{\ell=j+1}^{m} \frac{\partial\rho_a(r_i)}{\partial\rho_\ell} \right] (\rho_{j+1} - \rho_j) + \rho_1 \sum_{j=1}^{m} \frac{\partial\rho_a(r_i)}{\partial\rho_j}, \qquad i = 1, n, \quad \text{(A-4)}$$

which is the desired result.